

# A Novel Dimanganese(II) Complex with Two Chloride Bridges – A Two-Electron Oxidation System

Isabel Romero,<sup>[a]</sup> Marie-Noëlle Collomb,<sup>\*[a]</sup> Alain Deronzier,<sup>\*[a]</sup> Antoni Llobet,<sup>[b]</sup> Emmanuel Perret,<sup>[c]</sup> Jacques Pécaut,<sup>[c]</sup> Laurent Le Pape,<sup>[c]</sup> and Jean-Marc Latour<sup>\*[c]</sup>

**Keywords:** Manganese / N ligands / Biomimetic synthesis / Structure elucidation / Electrochemistry

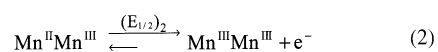
A new kind of binuclear  $\mu$ -chloro complex of manganese with two bpea ligands [bpea = *N,N*-bis(2-pyridyl methyl) ethylamine] has been synthesized and structurally character-

ized. A thorough electrochemical study shows that this complex exhibits a two-electron reversible oxidation leading to the stable dimanganese(III) complex.

## Introduction

One-electron transfers are ubiquitous in chemistry as well as in biology.<sup>[1]</sup> However, activation of diatomic substrates such as dioxygen and dinitrogen requires multielectron transfers, which are often performed by metal clusters at enzyme active sites.<sup>[2]</sup> Moreover, in specific instances, multi-electron transfers can be crucial because one-electron transfers may lead to deleterious effects. This is the case for catalases, the enzymes which carry out the disproportionation of hydrogen peroxide into water and molecular oxygen.

Most of these enzymes are hemoproteins, but a few bacterial catalases are known to possess a dinuclear manganese center at their active site.<sup>[3]</sup> It is generally believed that the Mn pair shuttles between the two oxidation states  $\text{Mn}^{\text{II}}\text{--Mn}^{\text{II}}$  and  $\text{Mn}^{\text{III}}\text{--Mn}^{\text{III}}$  during the catalytic cycle,<sup>[3a]</sup> thereby avoiding one-electron transfers which would produce hydroxyl radicals. The  $\text{Mn}^{\text{II}}\text{--Mn}^{\text{III}}$  mixed-valent state is never observed under the normal conditions where the catalase reaction occurs. The structure and mechanism of action of this active center remains poorly defined, and in order to gain insight into the structure and the disproportionation mechanism, many efforts have been devoted in the past decade to designing simple model molecules.<sup>[4]</sup> Many of these model systems contain two  $\text{Mn}^{\text{II}}$  ions bridged by ligands like carboxylate,<sup>[5]</sup> phenoxide,<sup>[6]</sup> alkoxide<sup>[7]</sup> or, more rarely, by chloride.<sup>[8]</sup> These compounds can undergo the two following distinct one-electron exchanges [Equation (1) and (2)]:



with formation of a mixed-valence  $\text{Mn}^{\text{II}}\text{--Mn}^{\text{III}}$  species<sup>[5]</sup> whose stability is expressed by the disproportionation constant ( $K_d$ ), determined from the separation of the redox potentials of the two one-electron steps. The stability of the mixed-valent state depends on the degree of electronic coupling of the two metal ions<sup>[9]</sup> and, for uncoupled metal ions, a direct two-electron redox transition at a single electrochemical potential is expected. It has been stressed recently that for dimanganese(II) species to achieve a high efficiency of catalase-like activity, formation of the mixed-valence  $\text{Mn}^{\text{II}}\text{--Mn}^{\text{III}}$  state must be disfavored.<sup>[3b]</sup> In this context, it is somewhat surprising that the electrochemical behavior of dimanganese  $\text{Mn}^{\text{II}}\text{--Mn}^{\text{II}}$  complexes has been only scarcely examined in detail. Indeed, only for three of these systems a direct two-electron redox transition has been proposed.<sup>[5c,8b,10]</sup> We report here the synthesis, crystal structure and magnetic properties of a new di- $\text{Mn}^{\text{II}}$  complex with a bis- $\mu$ -chloro unit  $\text{Mn}_2(\mu\text{-Cl})_2(\text{bpea})_2\text{Cl}_2$  (**1**) [bpea = *N,N*-bis(2-pyridylmethyl)ethylamine]. A thorough electrochemical study reveals that **1** exhibits a clean, two-electron reversible oxidation system leading to the stable di- $\text{Mn}^{\text{III}}$  complex.

## Results

### Solid State Structure

When  $\text{MnCl}_2$  dissolved in water was allowed to react with an ethanolic solution of the bpea ligand at ambient temperature, the colorless solution turned yellow and **1** could be crystallized by slow evaporation of the solution. The structure of this binuclear complex was determined by an X-ray crystallographic study (Figure 1).

<sup>[a]</sup> Laboratoire d'Electrochimie Organique et de Photochimie Rédox, UMR CNRS 5630, Université Joseph Fourier Grenoble 1, B. P. 53, 38041 Grenoble cedex 9, France

<sup>[b]</sup> Departament de Química, Universitat de Girona, Campus de Montilivi, E-17071 Girona, Spain

<sup>[c]</sup> DRFMC-Laboratoire de Chimie Inorganique et Biologique, UMR CEA-CNRS-UJF 5046, CEA-Grenoble, 38054 Grenoble Cedex, France

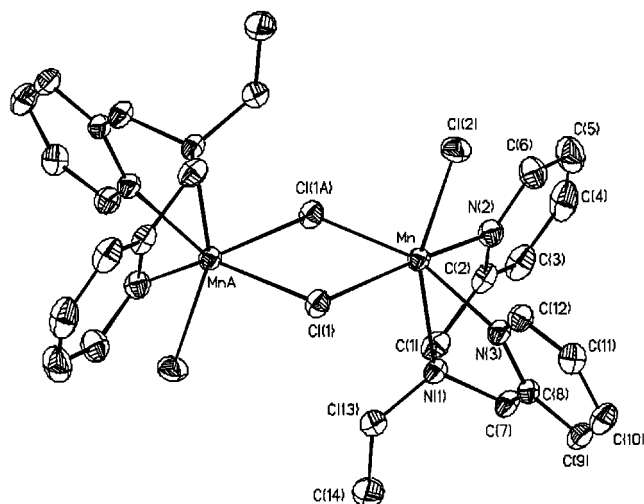


Figure 1. Molecular structure of **1**; selected bond lengths (Å) and angles (°): Mn–Mn#1 3.786, Mn–Cl(1) 2.5374(9), Mn–Cl(2) 2.4249(8), Mn–N(1) 2.4246(16), Mn–N(2) 2.2811(17), Mn–N(3) 2.2657(16), Mn–Cl(1) 2.5683(7); Mn(1)–Cl(1)–Mn#1 95.72(2), Cl(2)–Mn–Cl(1) 98.17(2), N(1)–Mn–Cl(1) 99.65(4), N(2)–Mn–Cl(1) 165.63(4), N(3)–Mn–Cl(1) 88.96(4), N(1)–Mn–Cl(2) 156.43(4), N(2)–Mn–Cl(2) 94.18(5), N(3)–Mn–Cl(2) 92.77(5), N(2)–Mn–N(1) 70.68(5), N(3)–Mn–N(1) 72.30(6), N(3)–Mn–N(2) 97.78(5), Cl(1)–Mn–Cl(1)#1 84.28(2), Cl(2)–Mn–Cl(1)#1 103.73(3), N(1)–Mn–Cl(1)#1 93.32(4), N(2)–Mn–Cl(1)#1 85.69(4), N(2)–Mn–Cl(1)#1 162.88(4)

Each Mn atom is bound by three nitrogen atoms from a facially coordinated bpea ligand, and three chloride ions, in an octahedrally distorted fashion. The two manganese atoms are bridged by a pair of chloride ions leading to an  $\text{Mn}_2\text{Cl}_2$  diamond core. The two manganese atoms are equivalent since the complex has a rotational  $C_2$  symmetry axis passing through the center of this core. Owing to the presence of the symmetry axis the  $\text{Mn}_2\text{Cl}_2$  core is strictly planar and the Mn–Mn bond length is 3.786 Å. The two Mn–Cl bridging bond lengths are slightly different [2.5374(8) and 2.5683(7) Å] and longer than the terminal Mn–Cl bond lengths (2.4249 Å). All these structural features are similar to those of other structurally characterized  $\text{Mn}^{\text{II}}\text{Mn}^{\text{II}}$  di- $\mu$ -chloro complexes.<sup>[10]</sup>

### Magnetic and Spectroscopic Properties

The temperature dependence of the product of the molar susceptibility and temperature ( $\chi T$ ) at 0.5, 1, 2.5 and 5 T is shown for **1** in Figure 2. In the range from 300 to 100 K,  $\chi T$  is constant at ca.  $8.5 \text{ cm}^3 \cdot \text{K} \cdot \text{mol}^{-1}$ , which is close to the value expected for two independent spins  $S = 5/2$  ( $8.75 \text{ cm}^3 \cdot \text{K} \cdot \text{mol}^{-1}$ ). At lower temperatures,  $\chi T$  increases to reach a maximum whose value and temperature depends on the applied magnetic field ( $11.5 \text{ cm}^3 \cdot \text{K} \cdot \text{mol}^{-1}$  at 4 K for 0.5 T,  $10.6 \text{ cm}^3 \cdot \text{K} \cdot \text{mol}^{-1}$  at 6 K for 1 T,  $9.9 \text{ cm}^3 \cdot \text{K} \cdot \text{mol}^{-1}$  at 14 K for 2.5 T and  $9.0 \text{ cm}^3 \cdot \text{K} \cdot \text{mol}^{-1}$  at 60 K for 5 T). This behavior is typical of a metal pair experiencing a ferromagnetic interaction. In those cases where the exchange interaction and the zero-field splittings are of comparable magnitudes, full diagonalization of the matrix is required to treat all field- and temperature-dependent data. Preliminary fit-

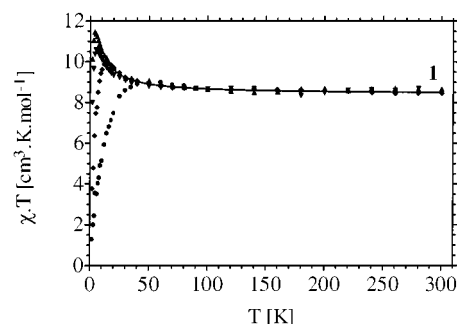


Figure 2. Temperature dependence of the product of the molar magnetic susceptibility and temperature for a microcrystalline sample of **1** ( $7.91 \times 10^{-5} \text{ mol}$  except at 2.5 T,  $6.60 \times 10^{-5} \text{ mol}$ ) at 0.5 (▲), 1 (▼), 2.5 (◆) and 5 T (●); solid line is the best least-square fit to the magnetic data

tings of the susceptibility data (Figure 2) with an expression based on a Heisenberg Hamiltonian ( $J = -2J S_1 S_2$ ), as described in the Experimental Section, were performed in the temperature range where the D effects are negligible. This led to an estimate of the magnetic exchange interaction of  $J = 0.34 (3) \text{ cm}^{-1}$ .

The solution EPR spectra have been recorded in dichloromethane (Figure 3) and in acetonitrile to investigate the nuclearity of the complex, either in the absence or presence of the electrolyte  $[(\text{nBu})_4\text{N}]\text{ClO}_4$  in order to duplicate the electrochemical conditions. The two spectra are essentially identical, which points to the absence of chemical change induced by the electrolyte. They exhibit features extending from 50 to more than 800 mT as is normal for dimanganese(II) species.<sup>[12]</sup> Nevertheless, owing to the fact that some distorted mononuclear manganese(II) compounds possess similar transitions,<sup>[13]</sup> the dinuclearity of the complexes in solution cannot be taken for granted on the basis of these spectra. We were definitely able to prove this, however, through the observation of intense EPR transitions in the parallel mode, a property expected only for integer spins<sup>[14]</sup> and which rules out that the active species is mononuclear. The EPR spectra in acetonitrile are quite similar, except for a minor amount of mononuclear decomposition products. Therefore the EPR study undoubtedly shows that **1** exists as a dinuclear entity in solution as well as in the solid state. The very small modification of the

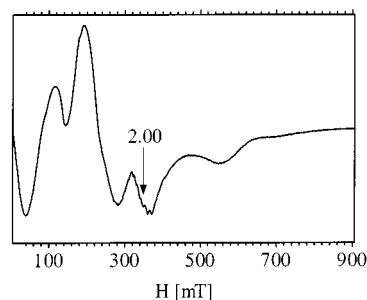


Figure 3. X-band EPR spectrum of **1** at a concentration of 1 mM in dichloromethane at 4.2 K; instrumental parameters: microwave frequency (9.6545 GHz), microwave power (0.2 mW), modulation amplitude (10 G), modulation frequency (100 kHz), sweep time 168 s; the six hyperfine lines centered at  $g \approx 2.02$  are attributed to a minor mononuclear Mn(II) impurity

whole spectrum shape with temperature in the range 3.8–50 K is in agreement with the small exchange-coupling obtained from magnetization measurements.

The dinuclearity of the complex in solution is shown again by an electrospray mass spectral study. Indeed, the compound appears as a complex pattern at  $m/z = 669$ – $677$  which corresponds to  $[(\text{bpea})\text{ClMn}(\mu\text{-Cl})_2\text{Mn}(\text{bpea})]^+$ . A theoretical mass analysis of the isotopic pattern confirms the presence of three chlorine atoms.

### Electrochemical Properties

The cyclic voltammogram (CV) of **1** ( $1 \times 10^{-3}$  M) in  $\text{CH}_3\text{CN}$  containing 0.1 M  $[(\text{nBu})_4\text{N}]\text{ClO}_4$  under Ar is shown in Figure 4. The CV exhibits a two-electron reversible oxidation wave corresponding to the  $\text{Mn}^{\text{II}}\text{Mn}^{\text{II}}/\text{Mn}^{\text{III}}\text{Mn}^{\text{III}}$  redox system ( $E_{1/2} = 0.63$  V;  $\Delta E_p = 80$  mV, scan rate =  $100 \text{ mVs}^{-1}$ ). A two-electron oxidation second wave only poorly reversible is also seen at  $E_{1/2} = 1.41$  V. The two-electron transfer nature of the waves is based on the intensity of the peaks compared to that of a one-electron transfer, and on coulometric experiments (v.i.). The first two-electron process [Equation (3)] can be decomposed in the two, reversible one-electron exchanges depicted in Equations (1) and (2) and the standard potentials ( $E_{1/2}$ )<sub>1</sub> and ( $E_{1/2}$ )<sub>2</sub> of each electron transfer can be calculated from the  $\Delta E_p$  of the overall process.<sup>[15]</sup> The values of ( $E_{1/2}$ )<sub>1</sub> and ( $E_{1/2}$ )<sub>2</sub> are 0.60 and 0.66 V, respectively, giving  $K_d = 1.2 \times 10^{-1}$ . These data indicate that the two one-electron transfers occur at similar potentials and that the mixed-valence species  $\text{Mn}^{\text{II}}\text{Mn}^{\text{III}}$  is only poorly stable.

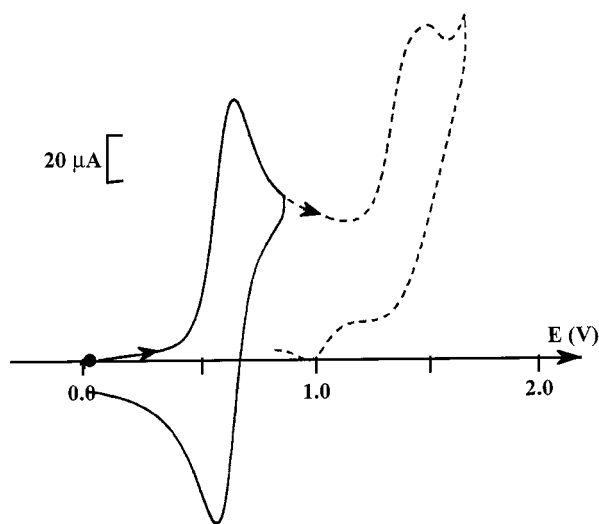
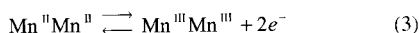


Figure 4. CV in  $\text{CH}_3\text{CN} + 0.1 \text{ M } [(\text{nBu})_4\text{N}]\text{ClO}_4$  of a 1 mM solution of **1** at a platinum electrode (5 mm diameter); scan rate:  $100 \text{ mV s}^{-1}$



The  $\text{Mn}^{\text{III}}\text{Mn}^{\text{III}}$  species could be prepared by an exhaustive electrolysis carried out at  $E_{\text{appl}} = 0.8 \text{ V}$  in  $\text{CH}_3\text{CN}$ . The initial yellow solution turned green-brown [ $\lambda_{\text{max}} = 416$  (shoulder) and  $534 \text{ nm}$ ]. The formation of a  $\text{Mn}^{\text{III}}\text{Mn}^{\text{III}}$

species is clearly demonstrated by voltamperometry experiments conducted at a Pt rotating disk electrode. After electrolysis, the anodic initial wave at  $E_{1/2} = 0.63$  V is retained as a cathodic one. However, the yield of  $\text{Mn}^{\text{III}}\text{Mn}^{\text{III}}$  species is only 85% as judged by a comparison of the height of the wave recorded before and after electrolysis. A slight excess of coulometry is observed (2.3 electrons per complex). EPR spectroscopy showed that the oxidized solution is EPR silent except for a small contribution from a mononuclear  $\text{Mn}(\text{II})$  decomposition product. It should be noted, however, that besides the  $\text{Mn}^{\text{III}}\text{Mn}^{\text{III}}$  complex, a species exhibiting a quasi reversible oxidation wave at  $E_{1/2} = 0.98$  V is generated in a 15% yield, as determined by the rotating disk experiment. No attempt has been made to identify this new species.

### Discussion

Electrochemical and spectroscopic studies have revealed that **1** exhibits reversible two-electron exchanges between dimanganese(II) and dimanganese(III) states. The latter state can be oxidized further in a two-electron process, but this transfer is less reversible. A two-electron oxidation of dimanganese(II) centers has been proposed recently for two complexes with aliphatic bridges.<sup>[5c][8b]</sup> This behavior is interpreted as arising from the independency of the two metal sites in agreement with an insulating effect of the aliphatic chain. In this respect, it is worth noting that the  $\Delta E_p$  of the overall process has been observed to decrease (from 128 to ca 75 mV) in dimanganese complexes of binucleating amine ligands when the length of the aliphatic chain distance increases from 2 to 3–4 methylene groups, and therefore the Mn–Mn distance from 6.3 to 8.3 Å.<sup>[8b]</sup> Such a two-electron transfer was proposed also for a  $(\mu\text{-alkoxo})(\mu\text{-acetato})$  compound<sup>[10]</sup> where the carboxylate was supposed to play a similar insulating role.<sup>[3b]</sup> Indeed the two sites must be electronically uncoupled in order not to bring any stabilization of the mixed-valent state. It therefore appears that in **1** the bridging chlorides, while structurally linking the two manganese ions, are actually isolating them electronically from one another. A comparison with the above-mentioned complexes reveals that in **1**, although  $\Delta E_p$  is small (80 mV), the Mn–Mn distance is short 3.8 Å, which points to a strong effect of the chloride bridges. This electronic uncoupling is reflected in the very weak magnetic coupling of the two Mn ions.

### Experimental Section

**General:** All syntheses and electrochemical experiments were performed under an argon atmosphere. Electrochemical equipment and procedures have been described previously.<sup>[16]</sup> Potentials are referred to an  $\text{Ag} | 10 \text{ mM } \text{Ag}^+$  reference electrode in  $\text{CH}_3\text{CN} + 0.1 \text{ M}$  electrolyte. The potentials referenced to that system can be converted into SCE by adding 300 mV. The bpea ligand was prepared following a literature method.<sup>[11]</sup>

**Mn<sub>2</sub>(μ-Cl)<sub>2</sub>(bpea)<sub>2</sub>Cl<sub>2</sub> (1):** To an aqueous solution (4 mL) of MnCl<sub>2</sub> (0.110 g, 0.88 mmol) was added an ethanol solution (4 mL) of bpea ligand (0.200 g, 0.88 mmol) with stirring. The resulting pale yellow solution was stirred for one hour, then filtered three times to remove any impurity and evaporated to dryness at room temperature. The white microcrystalline powder formed was redissolved in acetonitrile and colorless crystals were obtained by slow evaporation of this solution at room temperature. The crystals of **1** (0.125 mg, yield 40%) were collected by filtration, washed with diethyl ether and dried in air.

IR (KBr):  $\tilde{\nu}$  = 1600 (s), 1571 (m), 1475 (m), 1464 (w), 1432 (s), 1384 (m), 1361 (m), 1342 (w), 1303 (m), 1290 (m), 1268 (w), 1248 (w), 1211 (w), 1173 (w), 1150 (s), 1119 (m), 1099 (m), 1069 (w), 1044 (s), 1015 (s), 995 (m), 985 (w), 964 (w), 935 (w), 896 (w), 852 (w), 821 (m), 767 (s), 736 (w), 722 (w), 638 (m), 514 (w), 504 (w), 470 (w), 415 (m) cm<sup>-1</sup>. – C<sub>28</sub>H<sub>34</sub>Cl<sub>4</sub>Mn<sub>2</sub>N<sub>6</sub> (706.29): calcd. C 47.59, H 4.81, N 11.89; found C 47.29, H 4.79, N 11.72.

**X-ray Crystal Structure Analysis of 1:** C<sub>28</sub>H<sub>34</sub>Cl<sub>4</sub>Mn<sub>2</sub>N<sub>6</sub>,  $M$  = 706.29; monoclinic, space group  $P2_1/c$ ,  $a$  = 10.1085(19),  $b$  = 16.399(7),  $c$  = 10.089(3) Å,  $\alpha$  = 90,  $\beta$  = 109.771(17),  $\gamma$  = 90,  $V$  = 1573.9(9) Å<sup>3</sup>,  $T$  = 298(2) K,  $Z$  = 2,  $F(000)$  = 724,  $D_c$  = 1.490 g·cm<sup>-3</sup>,  $\mu$  = 1.171 mm<sup>-1</sup>. The data sets for the single-crystal X-ray studies were collected with Mo- $K_\alpha$  radiation on a Bruker SMART diffractometer. All calculations were performed on a Silicon Graphics system, using the SHELXTL program.<sup>[17]</sup> The structure was solved by direct methods and refined by full-matrix least-squares on  $F_2$ .

Crystallographic data (excluding structure factors) for the structure(s) included in this paper have been deposited with the Cambridge Crystallographic Data Centre as supplementary publication no. CCDC-146219. Copies of the data can be obtained free of charge on application to CCDC, 12 Union Road, Cambridge CB2 1EZ, UK [Fax: (internat.) + 44-1223/336-033; Email: deposit@ccdc.cam.ac.uk].

Magnetic measurements were performed using a Quantum Design MPMS SQUID magnetometer operating at 0.5–5 T over the temperature range 2–300 K. The powdered samples were contained in a kel-F bucket which was calibrated independently at the same fields and temperatures. The raw data were corrected for the sample holder contribution, and the molar susceptibility corresponds to the resulting magnetization per mol and per magnetic field unit. The subtracted diamagnetic contribution of **1** was evaluated at  $-429 \times 10^{-6}$  cm<sup>3</sup>·mol<sup>-1</sup>. The fitting procedure was effected in the range 12, 25, 60, 120–300 K at 0.5, 1, 2.5 and 5T, respectively. The fitting function, based on an Heisenberg Hamiltonian  $-2J S_1 \cdot S_2$ , was  $c [(1 - \alpha) 2Mn(II,II) + 8.75 \alpha] + 2TIP$ .  $T$ , with  $c$  to take into account uncertainties concerning the exact composition of the powder;  $2\alpha$ , the proportion of mononuclear Mn(II) seen by EPR;  $2Mn(II,II)$ , the Van Vleck formula for such a complex including parameters  $g$  and  $J$ , and  $TIP$  the Temperature Independent Paramagnetism and/or a ferromagnetic contribution.  $G$  was fixed to 2.

The fit gave  $J = +0.34$  (3) cm<sup>-1</sup>,  $c = 0.96$  (1),  $\alpha = 0$  (fixed) and  $TIP = 0$  (fixed).

Low temperature EPR spectra were recorded on an X-band Bruker EMX spectrometer equipped with an Oxford Instruments ESR-900 continuous-flow helium cryostat and an ER-4116 OM Bruker cavity. Magnetic field values were measured with an EMX-035M NMR gaussmeter.

Infrared spectra were recorded with a Perkin–Elmer Spectrum GX FTIR Spectrometer as KBr pellets.

- [1] S. Skourtis, D. N. Beratan, in *Electron Transfer in Chemistry* (Ed.: V. Balzani), Vol. 1, Wiley-VCH, in press.
- [2] R. E. Sharp, S. K. Chapman, *Biochim. Biophys. Acta* **1999**, *1432*, 143–158.
- [3] [3a] J. E. Penner-Hahn, in *Manganese Redox Enzymes* (Ed.: V. L. Pecoraro), VCH Publishers, New York, **1992**, pp 29–45. – [3b] G. C. Dismukes, *Chem. Rev.* **1996**, *96*, 2909–2926.
- [4] V. L. Pecoraro, M. J. Baldwin, A. Gelasco, *Chem. Rev.* **1994**, *94*, 807–826.
- [5] [5a] M. Devereux, M. Mc Cann, M. T. Carey, M. Curran, G. Ferguson, C. Cardin, M. Guvery, F. Quillet, *J. Chem. Soc., Dalton Trans.* **1995**, 771–776. – [5b] T. Tanase, S. J. Lippard, *Inorg. Chem.* **1995**, *34*, 4682–4690. – [5c] D. F. Xiang, X. S. Tan, W. T. Tang, F. Xue, T. C. W. Mak, *Polyhedron* **1998**, *17*, 1375–1380.
- [6] [6a] H. Okawa, H. Sakiyama, *Pure Appl. Chem.* **1995**, *67*, 273–280. – [6b] T. Nagata, J. Mizukami, *J. Chem. Soc., Dalton Trans.* **1995**, 2825–2830.
- [7] P. J. Pessiki, G. C. Dismukes, *J. Am. Chem. Soc.* **1994**, *116*, 898–903.
- [8] [8a] B. C. Unni Nar, J. E. Sheats, R. Pontecello, D. Van Engen, V. Petrouleas, G. C. Dismukes, *Inorg. Chem.* **1989**, *28*, 1582–1587. – [8b] S. J. Brudenell, L. Spiccia, A. M. Bond, G. D. Fallon, D. C. R. Hockless, G. Lazarev, P. J. Mahon, E. R. T. Tiekink, *Inorg. Chem.* **2000**, *39*, 881–892.
- [9] P. J. Pessiki, S. V. Khangulov, D. M. Ho, G. C. Dismukes, *J. Am. Chem. Soc.* **1994**, *116*, 891–897.
- [10] [10a] E. Sinn, *J. Chem. Soc., Dalton Trans.* **1975**, 162–165. – [10b] F. H. Köhler, N. Hebenanz, U. Thewalt, B. Kanellakopoulos, R. Klenze, *Angew. Chem. Int. Ed. Engl.* **1984**, *23*, 721–723. – [10c] A. Garoufis, S. Kasselouri, S. Boyatzis, C. P. Raptopoulou, *Polyhedron* **1999**, *18*, 1615–1620.
- [11] S. Pal, M. K. Chan, W. H. Armstrong, *J. Am. Chem. Soc.* **1992**, *114*, 6398–6406.
- [12] S. V. Khangulov, P. J. Pessiki, V. V. Barynin, D. E. Ash, G. C. Dismukes, *Biochemistry* **1995**, *34*, 2015–2025.
- [13] A. Bencini, D. Gatteschi, in *Transition Metal Chemistry* (Eds.: G. A. Mason and B. N. Figgis), Vol. 8, Chap. 1, M. Dekker, New York, **1982**.
- [14] A. Abragam, B. Bleaney, *Electron Paramagnetic Resonance of Transition Ions*, Clarendon Press, Oxford, **1970**.
- [15] D. Richardson, H. Taube, *Inorg. Chem.* **1981**, *20*, 1278–1285.
- [16] M. N. Collomb Dunand Sauthier, A. Deronzier, I. Romero, *J. Electroanal. Chem.* **1997**, *436*, 219–225.
- [17] G. M. Sheldrick, SHELXTL version 5.1. *An Integrated System for Solving, Refining and Displaying Crystal Structures from Diffraction Data*, Siemens Analytical X-ray Instruments, Madison, WI, **1990**.

Received July 3, 2000  
[100260]